Leaching Characteristics of Biomass Ash-Based Binder in Neutral and Acidic Media

Piyush Chaunsali[1, 2], Hugo Uvegi[1], Brian Traynor[1] and Elsa Olivetti[1]*
[1] Department of Materials Science and Engineering, MIT, Cambridge, USA 02139
[2] Department of Civil Engineering, IIT Madras, Chennai, India 600036

Piyush Chaunsali (pchaunsali@iitm.ac.in)
Hugo Uvegi (huvegi@mit.edu)
Brian Traynor (btraynor@mit.edu)
Elsa Olivetti (elsao@mit.edu), +16172530877

Acknowledgements

We would like to acknowledge the financial support for this research through the Tata Center for Technology and Design as well as the Environmental Solutions Initiative, both at Massachusetts Institute of Technology (MIT), Cambridge. We also acknowledge support from NSF CAREER #1751925 and partial support of the Government of Portugal through the Portuguese Foundation for International Cooperation in Science, Technology, and Higher Education, through the MIT Portugal Program. The authors thank Mr. Pankaj Agrawal of Bindlas Duplux Ltd. (Muzaffarnagar, India) for providing the materials used in this study. This work made use of the MRSEC Shared Experimental Facilities at MIT, supported by the National Science Foundation under award number DMR-1419807, and facilities at the Institute for Soldier Nanotechnologies (ISN) at MIT.

Leaching Characteristics of Biomass Ash-Based Binder in Neutral and Acidic Media

Piyush Chaunsali[1, 2], Hugo Uvegi[1], Brian Traynor[1] and Elsa Olivetti[1]*
[1] Department of Materials Science and Engineering, MIT, Cambridge, USA 02139
[2] Department of Civil Engineering, IIT Madras, Chennai, India 600036

Abstract

Biomass ash results from the combustion of agricultural residues, which, in many developing countries, are a primary source of power generation for small and medium size industries. This study focuses on the performance of a binder synthesized from an Indian biomass ash, Indo-Gangetic clay, hydrated lime, and aqueous 1M NaOH solution. To measure the extent of leaching and its impact on physicochemical properties, the biomass ash binder in powder form (<45 μm size) was exposed to two different leaching media: deionized water and 0.1M HNO_3 at two different solution-to-sample ratios (by wt.) of 10 and 100. Sodium leaching was found to be prominent in the biomass ash binder irrespective of leaching medium and solution-to-sample ratio. However, calcium leaching was significantly higher in 0.1M HNO_3 than in deionized water. Calcium silicate hydrate present in the biomass ash binder was found to be less chemically stable in 0.1M HNO_3, exhibiting complete calcium leaching at a solution-to-sample ratio of 100. Furthermore, significant leaching of calcium in 0.1M HNO_3 solution resulted in phase modification of calcium silicate hydrate, the main reaction product of the biomass ash binder.

Keywords: Biomass ash; Clay; Pozzolanicity; Alkali desorption; Alkali-activation; Nitrogen sorption

1 Introduction

Biomass is an attractive energy source due to its apparent environmental benefit over fossil fuels. Globally, bioenergy accounted for 10% of the world's energy consumption in 2011 [1]. Over the past few years, biomass incineration for electricity generation has increased in many of Asia and Africa's developing nations, resulting in significant residual biomass ash [1]. Silica-rich material, such as rice husk ash, has proven useful as a precursor for both calcium silicate hydrate-based and sodium aluminosilicate-based binders [2-11]. Aqueous alkaline solutions, containing hydrated lime and/or alkali hydroxide, facilitate the dissolution of alumina and silica from biomass ash. Previous studies by the authors, which focused on beneficial use of local materials, demonstrated a low-energy process for effective use of biomass ash in the synthesis of a cementitious binder [12, 13].

In these studies, the binder was produced from an Indian biomass ash (70% by wt.), Indo-Gangetic clay (20% by wt.) and hydrated lime (10% by wt.) as the precursor materials, and aqueous sodium hydroxide solution as the activating solution. Compressive strength of this binder ranged from 10–15 MPa after 28 days at near-ambient temperature [12]. A detailed characterization of the reaction product in the biomass ash binder indicated the formation of calcium silicate hydrate (C-S-H), which is also the main hydration product of Portland cement [13]. Residual unburnt carbon present in the biomass ash poses a challenge for its beneficial use in cementitious materials as higher carbon content has been observed to lead to increased adsorption of air entraining admixtures and higher water demand [14, 15].

In this contribution, we explore the physicochemical properties of a biomass ash binder after long exposure to neutral and acidic media. Although these binders exhibit requisite strength for

structural application [16], the use of alkali-rich solutions (i.e. NaOH) in binder synthesis demands investigation into what, if any, effect alkali leaching might have on binder structural integrity. The main reaction product of this binder has a low Ca/Si ratio, and there are limited previous studies on the leaching behavior of such systems [17, 18]. As alkali leaching from the reaction product is of primary interest here, some earlier studies in the areas of alkali binding and leaching are summarized in the following paragraph.

Alkali binding of calcium silicate hydrates has been the topic of research in several previous studies [17-21], most of which have focused on estimating the alkali binding potential of synthetic C-S-H gels in alkaline solutions of known concentration. Stade [19], L'Hôpital et al. [20], and Hong and Glasser [21] studied alkali binding of C-S-H products with Ca/Si ratios in the range of 0.6-1.8 and all observed higher sorption at lower Ca/Si. At low Ca/Si, C-S-H has been shown to exhibit a greater fraction of acidic silanol (Si-OH) surface species, which can easily be deprotonated and charge compensated by available alkali species [19-21]. Hong and Glasser [21] also examined the desorption behavior of alkalis from synthesized C-S-H gels which were initially used for sorption experiments. The extent of alkali desorption ranged from 55–70% of initial alkali content of C-S-H. Swanton et al. [18] studied the dynamic leaching behavior of C-S-H gels with low Ca/Si ratio (0.2–0.6) and reported that C-S-H gels with Ca/Si > 0.29 evolve, on leaching, towards a congruent point with a Ca/Si ratio close to 0.84, whereas C-S-H gels with Ca/Si < 0.29 become increasingly silica-rich on leaching.

There are limited studies on the durability of biomass ash-based binders with respect to their leaching characteristics. This work examines the leaching behavior of a biomass ash binder in neutral and acidic media. More specifically, this paper reports the extent of elemental (Na, Ca and Si) leaching from the biomass ash binder, and its associated impact on mineralogy and

microstructure. Since the pH difference between the alkaline pore solution of the binder and the leaching solution drives the leaching process, two solutions (pH ~1.2 and ~7.3) were selected to capture the extent of leaching from the biomass ash binder.

Given conditions more extreme than those experienced in real-world application, this study aims to illustrate the maximum possible leaching of Na, Ca, and Si from such a biomass ash binder. These results are important for both structural and environmental considerations. Leaching of free alkalis has previously been shown to affect surrounding ecology [22], while decalcification and silica leaching have been shown to detrimentally affect the strength of similar C-S-H based binder products [23, 24]. Freely available alkalis (i.e. those not bound in the binder) also pose a risk for formation of alkali silica gel, which in turn, can also lead to structural degradation [25]. By exposing the biomass ash binder to simulated conditions similar to and more extreme than those experienced under ambient climatic conditions, we can observe an upper bound for the extent of possible leaching. A field study on a pilot biomass ash brick wall in Muzaffarnagar, India was conducted to relate the effects of ambient climatic conditions to lab observations.

2 Materials and Methods

2.1 Materials

An Indian biomass ash (source: Silverton Pulp & Papers Pvt. Ltd., Muzaffarnagar, India), derived from the burning of a mix of rice husk and sugarcane bagasse, was used in this study. Table 1 shows the oxide composition of the Silverton ash as determined by X-ray fluorescence (XRF) using ASTM C311, also highlighting its high loss-on-ignition value (LOI). As shown in Figure 1, X-ray diffraction (XRD) analysis of Silverton ash revealed phases such as quartz, albite, cristobalite, sylvite, and arcanite [12, 13]. The phase composition of Silverton ash, as calculated previously by quantitative XRD [13], showed ~90% amorphous content which also

accounts for the contribution of the amorphous unburnt carbon present in the ash. Clay from the Indo-Gangetic Plain was also used in this study and was largely crystalline, as evident from the XRD pattern in Figure 1. The amorphous content of clay was lower (~20%) compared to Silverton ash. Powder diffraction files used for XRD pattern fitting are provided in Table 2. The d_{10}, d_{50} and d_{90} particle sizes of ash were ~23 µm, ~92 µm, and ~240 µm, respectively. Clay had d_{10}, d_{50} and d_{90} particle sizes as ~2.8 µm, ~22 µm, and ~256 µm, respectively.

Table 1 Chemical composition (oxide %) of biomass ash and clay using XRF

Oxide (%)	SiO_2	Al_2O_3	Fe_2O_3	SO_3	CaO	Na_2O	MgO	K_2O	P_2O_5	Trace*	LOI#
Ash	61.73	1.12	0.63	1.96	1.6	0.17	0.81	2.22	0.86	0.15	26%
Clay	71.7	13.3	5.03	0.02	0.77	0.96	1.51	2.53	0.07	0.76	0.5%

* Includes TiO_2 MnO_2, BaO, and SrO; #loss-on-ignition (LOI) at 750 °C

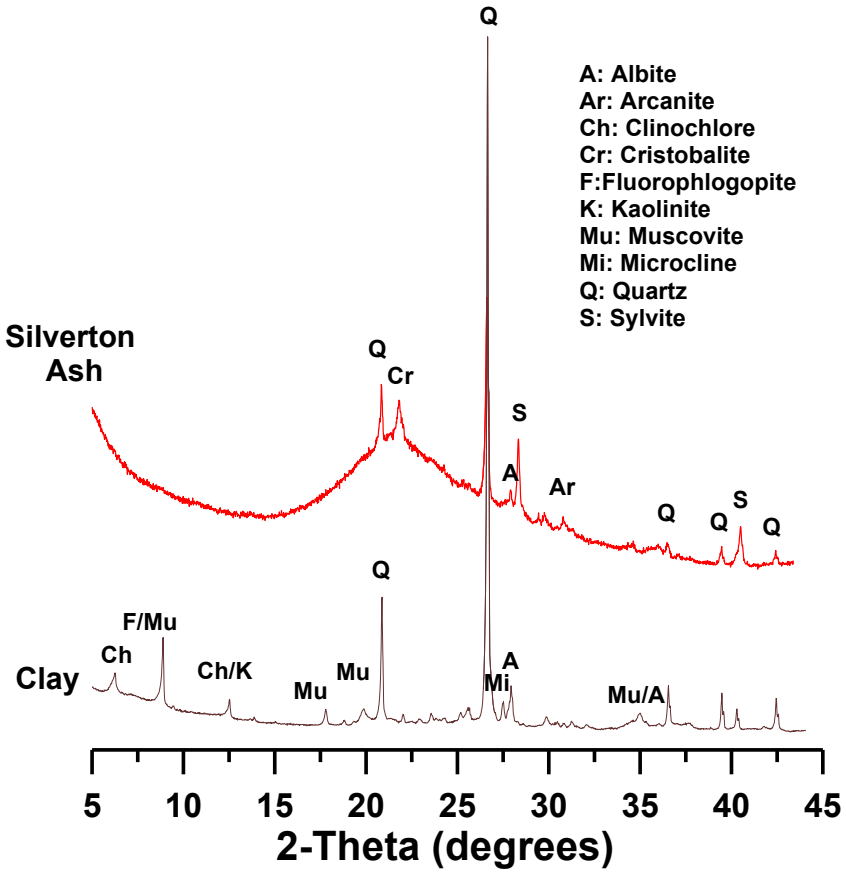

Figure 1. X-ray diffraction patterns of Silverton ash and clay

Table 2 Crystalline phases observed in XRD and corresponding powder diffraction files

Crystalline Phase Observed	**Powder Diffraction File (ICDD PDF 4+ 2019)**
Albite	00-009-0466
Arcanite	04-005-7905
Chlinoclore	04-011-2553
Cristobalite	04-008-7641
Fluorophlogopite	00-016-0344
Kaolinite	04-013-3074
Muscovite	01-073-9861
Microcline	04-011-0526
Quartz	00-046-1045
Sylvite	04-007-9713

2.2 Sample preparation

Biomass ash, clay, and hydrated lime (i.e., $Ca(OH)_2$) were proportioned (by wt.) at 70%, 20%, and 10%, respectively. For sample preparation, biomass ash and clay having a maximum particle size of 500 μm were used. Further details on the optimization of the mixture proportion development can be found in Laracy's work [26]. Sodium hydroxide (NaOH) solution of 1 mol/L (M) concentration was used as an activating solution, prepared by dissolving NaOH pellets (Macron Fine Chemicals, ≥ 98% assay) in deionized water. The liquid-to-solid (L/S) ratio was 0.40 for all mixtures. The mixing was performed in a Kitchen Aid mixer at the maximum speed (~220 rpm) for 15 minutes. Samples were then hydraulically pressed into 200 gram cubes, compacted using a Baldwin Tate Emery Universal Testing Machine to final pressures of 10 MPa with a fixed loading rate of 15000 N/min. The compaction mold had inner cross-sectional dimensions of 50 mm × 50 mm. The height of compacted samples was ~50 mm. Subsequently,

samples were wrapped in plastic sheet and stored in an oven operating at 30°C ± 2°C for at least the initial 7 days of curing.

2.3 Leaching test

Leaching behavior is influenced by the sample size such that the leaching process becomes diffusion-controlled as sample size increases. In order to mitigate the diffusion related issues, powdered samples were prepared by grinding bulk samples. After 7 days of initial curing, binder samples were ground to a particle size of less than 45 μm. Before beginning the leaching test, samples were dried in a vacuum desiccator at 20°C ± 2°C for 24 hours. Leaching tests were carried out in two solutions: deionized water (pH ~7.3) and 0.1M HNO_3 (pH ~1.2). These two solutions were used to capture the range of leaching extent of various elements from the biomass ash binder. The samples were weighed after 24 hours in a desiccator and immersed in one of the two solutions (acidic or neutral) at solution-to-sample ratios (by wt.) of 10 and 100. Five samples were prepared for each batch to determine the extent of leaching. To expedite leaching, the samples were continuously agitated in an orbital shaker at 140 rpm. After 28 days and 90 days of soaking, leachate solution was analyzed using inductively coupled plasma optical emission spectrometry (ICP-OES) for various elemental species. Leached and unleached powders were soaked in isopropyl alcohol for 24 hours, and subsequently dried in a vacuum desiccator for at least 24 hours. The drying method affects the pore structure and phase stability as reported in earlier studies [27, 28]. The present study employed solvent exchange followed by a low vacuum drying deemed reasonable for characterization [29, 30]. The dry powders (leached and unleached) were analyzed using nitrogen sorption for monitoring the changes in cumulative pore volume. Moreover, X-ray diffraction (XRD), thermogravimetric analysis (TGA), and Fourier

transmission infrared spectroscopy (FTIR) were used to monitor the changes in phase composition.

2.4 Inductively coupled plasma optical emission spectrometry (ICP-OES)

An Agilent 5100 Vertical Dual View ICP-OES with an auto-sampler was used to analyze reactant dissolution. Calibration standards were prepared from a standard solution containing 1000 ppm of Ca, Al, Si, Na, and K elements (Elemental Scientific, Omaha, NE) using 2% HNO_3 solution (prepared from TraceSELECT HNO_3 and ACS reagent grade water) for dilution.

2.5 Thermogravimetric analysis (TGA)

Thermogravimetric analysis was performed to determine the bound water content of reaction product on 25 ± 2 mg of powdered samples (< 45 μm size) using a Q50-TA Instrument. The samples were heated in a nitrogen environment (flow: 50 ml/min) up to 900°C at the rate of 15°C per minute.

2.6 X-ray diffraction (XRD)

X-ray diffraction data was collected using high speed Bragg-Brentano optics on a PANalytical X'Pert Pro MPD operated at 45 kV and 40 mA. CuKα source of wavelength 1.5405Å was employed in XRD measurements. The diffraction patterns were obtained for different 2-Theta ranges: 5°–70° and 20°–35° using step size of 0.0167° and 0.008°, respectively. The diffractometer settings (i.e., sizes of divergent slit, soller slit, and anti-scatter slit) were optimized according to 2-Theta range and sample holder size.

2.7 Fourier transform infrared spectroscopy (FTIR)

FTIR spectroscopy was performed using a Thermo Scientific Nicolet 6700 Fourier transform infrared spectrometer. Transmission spectra were collected from 4000 to 400 cm^{-1} with a

resolution of 2 cm^{-1}. Samples were run using the KBr pellet method, with approximately 1mg of sample blended with 400 mg of KBr matrix immediately prior to measurement.

2.8 Nitrogen sorption test

Nitrogen adsorption and desorption isotherms of dry powders (leached and unleached) were obtained at 77 K on a Micromeritics ASAP 2010 system. Before the measurement, samples were degassed at 50°C under vacuum for several hours. The Barrett-Joyner-Halenda (BJH) theory was used to evaluate the pore size distribution from the adsorption isotherm of powdered sample.

3 Results and discussion

This section examines the properties of the biomass ash binders after 28 days of leaching duration in either deionized water or 0.1M HNO_3 solution. The extent of leaching and its associated impact on the binder's mineralogical and microstructural characteristics are discussed in the following sections.

3.1 Leaching characteristics: Influence of the leaching medium and solution-to-sample ratio

Extent of leaching from the biomass ash binder was found to be dependent on leaching solution pH. As expected, larger pH gradient between the sample pore solution and leaching solution resulted in a higher degree of leaching. Figure 2 shows that the degree of elemental leaching (Na, Ca, and Si) was higher in 0.1M HNO_3 solution than in deionized water. Furthermore, higher solution-to-sample ratio (i.e., 100) increased the extent of leaching. The degree of sodium leaching at solution-to-sample ratio of 10 was ~87% and ~100% of total available sodium (normalized by the dry wt. of binder) in deionized water and 0.1M HNO_3, respectively. Furthermore, sodium leaching for solution-to-sample ratio of 100 increased to ~93% and ~100% in DI water and 0.1M HNO_3, respectively. This observation is consistent with previous studies which have reported alkali desorption from synthesized C-S-H gels. Hong and Glasser (1999)

found that alkali (Na and K) desorption from synthesized C-S-H with 0.85 Ca/Si ranged from 55% to 70% in pure water [21]. Similarly, Bach et al. reported 70–95% desorption of sodium from a low-pH cement after 12 months of curing in pure water at 20°C [31]. Significant alkali leaching in both this study and those cited above is the result of alkalis being either loosely bound in the C-S-H phase or remaining as residual salts post-sample drying. This is in contrast to geopolymeric binders, which are mainly comprised of sodium aluminosilicate phase with strongly bound sodium in its network-like structure. Zhang et al. [32] measured the extent of alkali leaching from fly ash-based geopolymers and reported less than 16% sodium leaching when the activator solution was either sodium hydroxide or sodium silicate solution.

As opposed to alkali leaching, calcium leaching was minimal (< 5%) after 28 days of soaking in DI water. While alkalis may be loosely bound to surface sites, calcium is structurally bound in the C-S-H phase. This is further verified by the difference in calcium leaching between the two leaching solutions. Calcium leaching was two orders of magnitude higher in 0.1M HNO_3 than in DI water due to higher pH gradient and lower chemical stability of C-S-H in acidic environments. It is evident from Figure 2 that the 0.1M HNO_3 destroys the C-S-H structure, leading to higher calcium leaching. After 28 days in 0.1M HNO_3, calcium present in biomass ash binder completely leached out at the solution-to-sample ratio of 100. However, silicon leaching was quite minimal (i.e., < 6%) irrespective of leaching medium and solution-to-sample ratio. The results of our study are consistent with a previous study by Shi and Stegemann [33] who reported that acid solutions with lower pH resulted in higher corrosion of cement pastes, calcium being more sensitive to the pH drop than Si. Long-term leaching tests revealed that there was no significant difference in the degree of leaching between 28 days and 90 days of soaking.

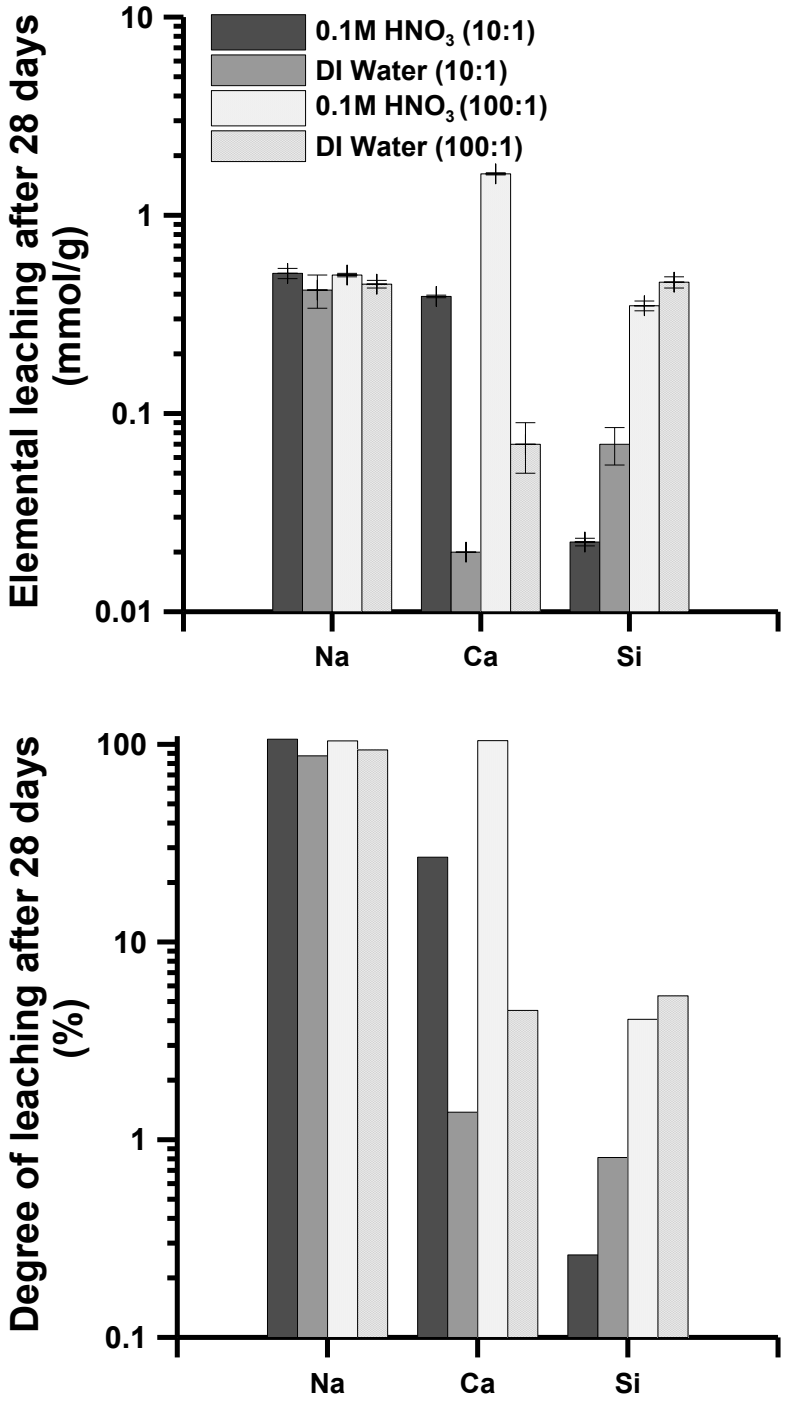

Figure 2. Influence of leaching medium and solution-to-sample ratio on extent of leaching from biomass ash binder (Note: leaching duration – 28 days)

3.2 Characterization of reaction product using XRD, FTIR, and TGA

The main binding phase in the biomass ash binder was found to be calcium silicate hydrate (C-S-H) as evident from the XRD patterns in Figure 3(a). Although the samples in HNO_3 at solution-

to-sample ratio of 10 had lost a portion (~27%) of the calcium from C-S-H, as evident from ICP results in Figure 2, the C-S-H peak could still be observed, as shown in Fig 3(b). The short range (28–32° 2θ) XRD patterns in Figure 3(b) indicate that the leaching in deionized water and HNO_3 solution led to narrowing of the peak width at solution-to-sample ratio of 10. Such narrowing is indicative of two possible scenarios. First, narrow XRD peaks typically correspond to larger crystallite sizes, as indicated by the inverse relationship between peak width and crystallite size given by the Scherrer equation [34, 35]. Alternatively, by examining the XRD peak positions of crystalline calcite (PDF: 00-005-0586) and different tobermorite patterns (PDFs: 04-011-0271, 04-012-1761), the latter of which can be taken as a stand-in for the synthesized C-S-H, it is quite possible that the dissolved Ca derives from the C-S-H phase, while any calcite present is less affected at such dilution. Crystallite growth is more likely in DI water, as hydration could possibly continue in the presence of such water. The latter is more likely in 0.1M HNO_3, as indicated by the observation of minimal leaching. In 0.1M HNO_3, however, the solution-to-sample ratio of 100 completely destroyed the C-S-H structure as well as any calcite present, yielding no observable peak between 28–32° 2θ, as shown in Figure 3(c). The long-term experiments revealed that the C-S-H phase in biomass ash binder was stable in deionized water even after 90 days of leaching and may even become further hydrated. Continuous presence of C-S-H in DI water-leached samples can be attributed to minimal calcium leaching, as observed in Figure 2.

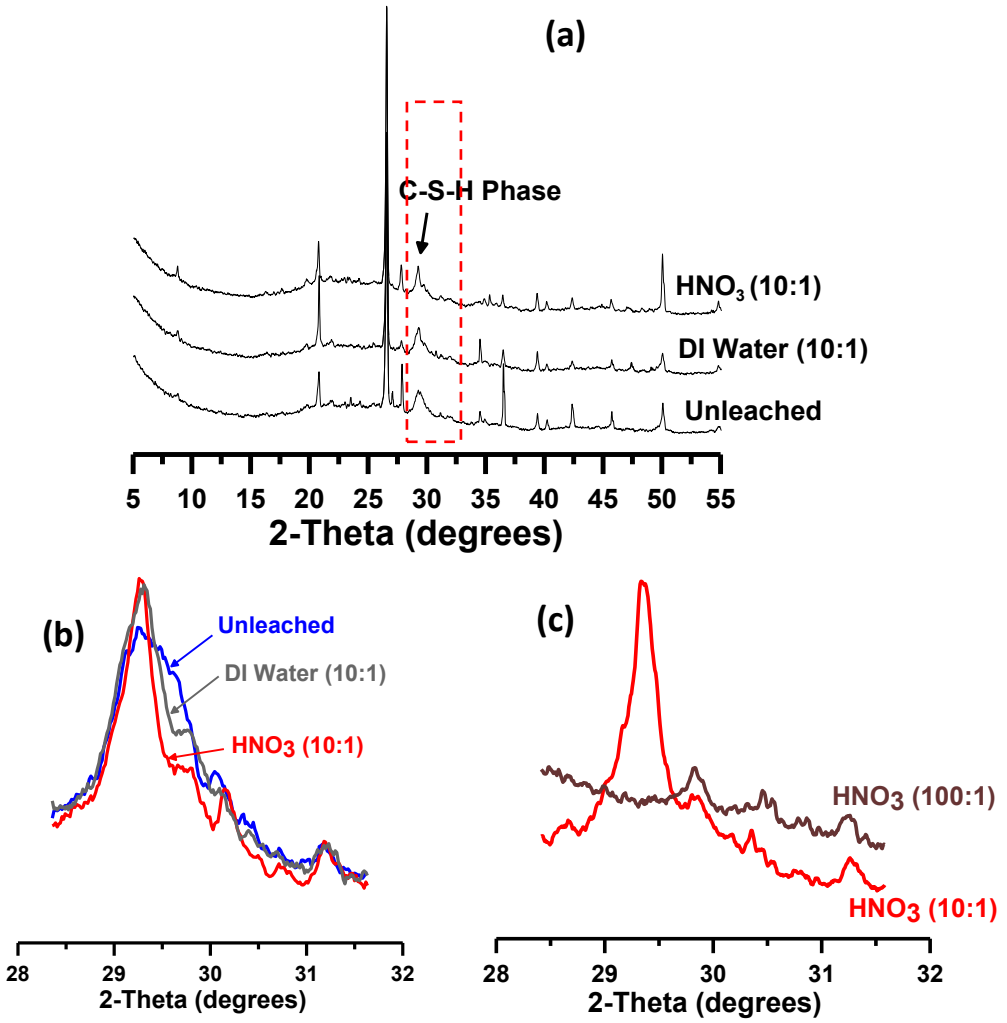

Figure 3 (a)-(c) X-ray diffraction patterns of unleached and leached samples (Note: leaching duration – 28 days)

Due to the overlap between the C-S-H and calcite peaks in XRD, FTIR analysis was performed to monitor the changes in C-S-H phase. FTIR spectra also revealed changes in bonding environment of C-S-H phase after leaching. The peak at ~968 cm^{-1} is associated with the Si-O stretching vibrations of C-S-H gel [36]. The change in the peak at ~968 cm^{-1} after leaching in HNO_3 solution is evident in Figure 4. Samples leached in deionized water exhibited minimal change in comparison to HNO_3 leached samples. The DI water-leached samples had a distinct C-S-H signature even at high solution-to-sample ratio (i.e., 100). On the other hand, 0.1M HNO_3

was found to be detrimental to the C-S-H phase with complete disappearance of the C-S-H phase at high solution-to-sample ratio, confirming observations made by XRD.

The presence of unreacted phases (biomass ash and clay) was verified by comparing the FTIR spectra of raw materials and leached binders (data not shown here). These results indicate that although the binder consists of unreacted ash and clay in addition to the C-S-H reaction product, observed leaching is derived from the C-S-H phase.

It is noted that while the IR spectra were collected from 400-4000 cm^{-1}, no major differences between leached and unleached samples were observed in regions other than the 900-1200 cm^{-1} section, reminiscent of asymmetric Si-O stretching vibration, presented in Figure 4. Other bands observed in all spectra are as follows: a small peak was at 3642 cm^{-1} due to -OH in $Ca(OH)_2$, bands at 3450 cm^{-1} and 1633cm^{-1} due to H_2O, a broad band around 1450 cm^{-1} due to -CO in $CaCO_3$ and bands at 792 cm^{-1} and 462 cm^{-1} due Si-O in the precursor ash.

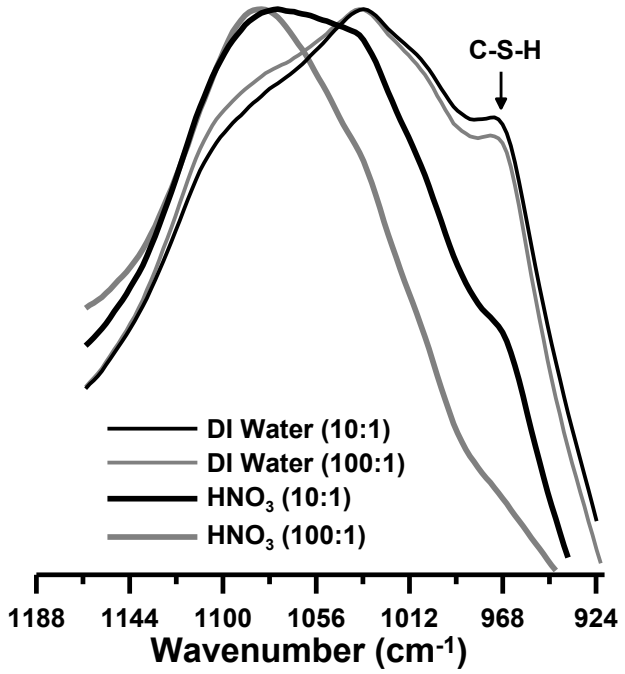

Figure 4. FTIR analysis of leached samples after 28 days of leaching

The difference between HNO_3-leached and unleached samples becomes more evident in the thermogravimetric analysis. No significant change in weight loss was observed between the unleached and the DI water-leached samples whereas the difference in weight loss of HNO_3-leached sample and others is quite evident in Figure 5. The extensive calcium leaching is detrimental to the structure of C-S-H phase and the reduced weight loss in the range of 50–800°C highlights this phenomenon [37]. Due to the absence of portlandite and minimal carbonation of binders (unleached and leached) after 28 days of leaching, the weight loss in the range of 50–800°C can be attributed to the change in bound water content of the C-S-H phase. The results from XRD, TGA, and FTIR analyses emphasize that deionized water did not affect the stability of C-S-H phase, but the exposure to 0.1M HNO_3 solution led to changes in C-S-H phase depending on the solution-to-sample ratio.

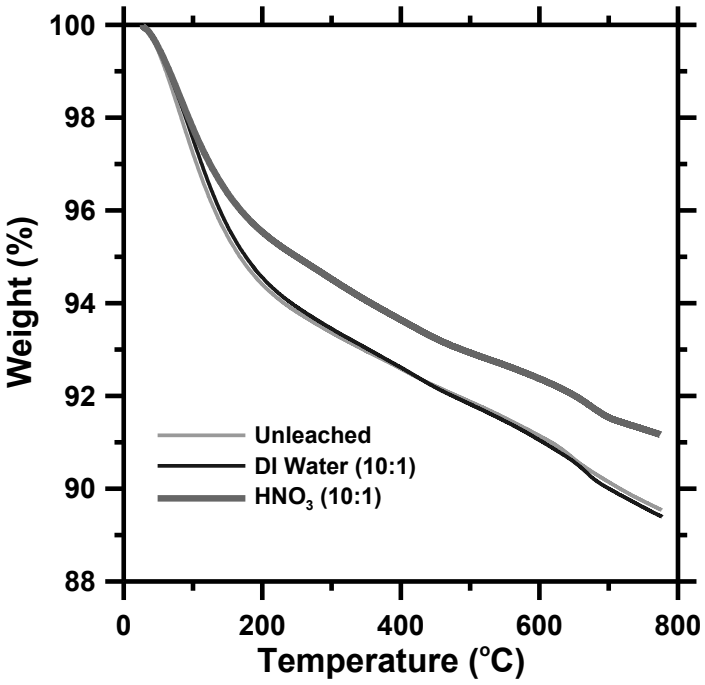

Figure 5. Thermogravimetric analysis of unleached and leached samples at solution-to-sample ratios of 10 (Note: leaching duration – 28 days)

3.3 Pore structure features determined using Nitrogen adsorption test

In order to examine whether leaching yielded a change in microstructure, nitrogen adsorption and desorption isotherms were obtained on leached and unleached samples. Figure 6 (a) shows the adsorption-desorption isotherms of leached and unleached samples. An upward shift in adsorbed volume of nitrogen suggests a change in pore structure features. The pore size distribution was estimated using the adsorption isotherm. Cumulative pore volume as plotted in Figure 6 (b) indicates that the leaching led to higher cumulative pore volume. Leaching of various elements from the reaction product led to increased porosity in the range of 1–300 nm which was captured in nitrogen sorption test. The BET surface area values for unleached, DI water-leached and HNO_3-leached samples were estimated as ~ 37 m^2/g, ~ 60 m^2/g and ~ 43 m^2/g, respectively. Similarly, BET surface area after leaching was at least 15% higher than before leaching. In this study, leaching resulted in an increase in surface area and cumulative pore volume, which was in accordance to the findings of Hidalgo et al. [38]. The effect of DI water and 0.1M HNO_3 was found to be similar on cumulative pore volume when solution-to-sample ratio was 10. It appears that the combined leaching of alkalis and calcium primarily dominated the change in pore structure in spite of higher calcium leaching (~20%) in case of 0.1M HNO_3.

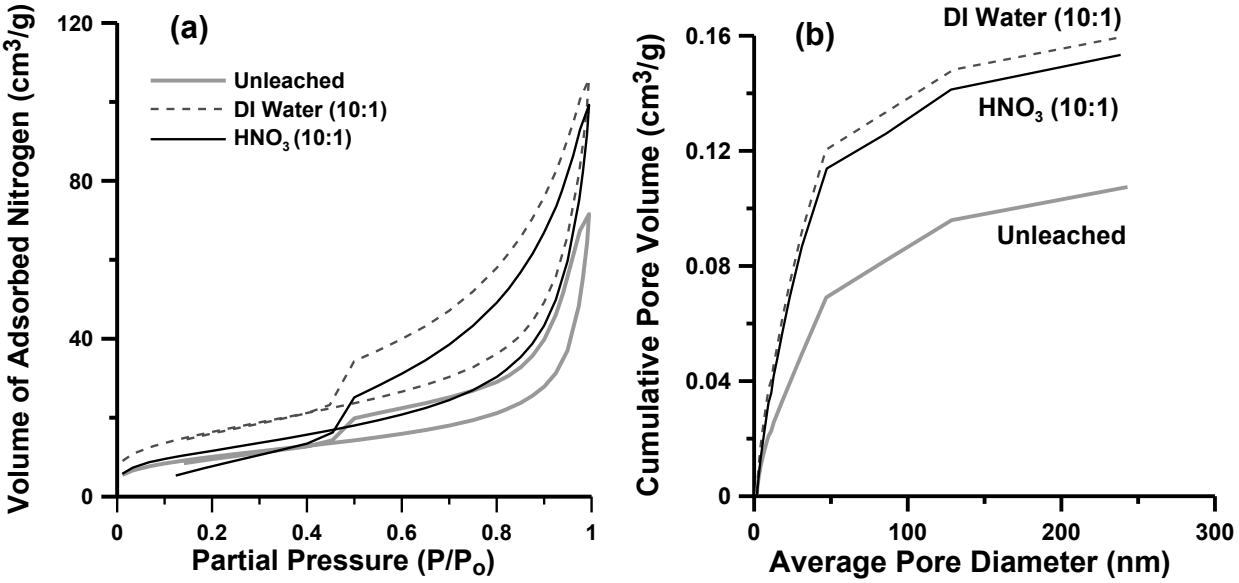

Figure 6 (a) BET adsorption-desorption isotherms, and (b) cumulative pore volume of leached and unleached samples (Note: leaching duration – 28 days)

3.4 Field application of biomass ash binder

In the current study, the biomass ash binder exhibited good resistance when exposed to deionized water irrespective of solution-to-sample ratio. This result has been confirmed by field observations on the durability of a pilot biomass ash brick wall. A wall made with biomass ash bricks (location: Muzaffarnagar, India) did not undergo any deterioration after long-term field exposure (1+ years). Figure 7 shows a photograph of the brick wall made of biomass ash binder. Closer examination of the bricks from the wall revealed no damage from cracking or efflorescence. Calcium silicate hydrate having a low Ca/Si ratio appeared to have shown enhanced chemical resistance in deionized water. However, significant calcium leaching was observed in acidic medium. As reported above, most of the calcium present in the biomass ash binder was found to have leached out in 0.1M HNO_3 at solution-to-sample ratio of 100.

Figure 7. A brick wall prototype (left) and two bricks (right) made of 1M NaOH-activated biomass ash binder (Note: The wall was built in Muzaffarnagar, India in July 2017)

It is acknowledged that higher solution-to-sample ratio than currently used in this study (10:1 and 100:1) will further increase the extent of leaching. However, our main observations regarding the fast removal of alkalis and higher calcium leaching in acidic medium are expected to be valid. The leaching experiments performed on powdered samples present the extreme case of the leaching phenomenon. In field application, leaching characteristics will also depend on the size of the structural element which will govern the diffusion kinetics as well as any additives or coatings employed.

4 Conclusions

In this study, the performance of an Indian biomass ash binder was evaluated in deionized water and 0.1M HNO_3 solution. The extent of leaching (both sodium and calcium) was found to be higher in 0.1M HNO_3 solution than in deionized water. Most of sodium (i.e. 85–100%) leached out of the biomass ash binder, indicating its loosely bound or unbound/residual nature. Calcium leaching was significant in 0.1M HNO_3 solution which resulted in modification and destruction of the main C-S-H product phase. The treatment in 0.1M HNO_3 solution at solution-to-sample ratio of 100 resulted in complete removal of calcium from the binder. These results indicate that

while the C-S-H binding phase would maintain stability in field conditions (i.e. exposure to relatively neutral pH water in the form of rain), sodium leaching is a concern. Further investigation into use of lower molarity sodium hydroxide should be conducted to minimize sodium leaching into the surrounding environment during field use.

Acknowledgements

We would like to acknowledge the financial support for this research through the Tata Center for Technology and Design as well as the Environmental Solutions Initiative, both at Massachusetts Institute of Technology (MIT), Cambridge. We also acknowledge support from NSF CAREER #1751925 and partial the support of the Government of Portugal through the Portuguese Foundation for International Cooperation in Science, Technology, and Higher Education, in the MIT Portugal Program. The authors thank Mr. Pankaj Agrawal of Bindlas Duplux Ltd. (Muzaffarnagar, India) for providing the materials used in this study. This work made use of the MRSEC Shared Experimental Facilities at MIT, supported by the National Science Foundation under award number DMR-1419807, and facilities at the Institute for Soldier Nanotechnologies (ISN) at MIT.

Conflicts of interest

The authors declare no conflicts of interest.

References

[1] World Energy Resources, Bioenergy, 2016. https://www.worldenergy.org/wp-content/uploads/2017/03/WEResources_Bioenergy_2016.pdf (accessed on Sept 1, 2018).

[2] S. V. Vassilev, D. Baxter, L. K. Andersen, C. G. Vassileva, An overview of the composition and application of biomass ash. Part 1. Phase–mineral and chemical composition and classification, Fuel. 105 (2013) 40-76.

[3] S. A. Bernal, E. D. Rodríguez, R. M. de Gutiérrez, J. L. Provis, S. Delvasto, Activation of metakaolin/slag blends using alkaline solutions based on chemically modified silica fume and rice husk ash, Waste Biomass Valori. 3 (2012) 99-108.

[4] N. Billong, U. Melo, E. Kamseu, J. Kinuthia, D. Njopwouo, Improving hydraulic properties of lime–rice husk ash (RHA) binders with metakaolin (MK), Constr. Build. Mater. 25 (2011) 2157-2161.
[5] P. Duxson, A. Fernández-Jiménez, J. L. Provis, G. C. Lukey, A. Palomo, J. Van Deventer, Geopolymer technology: the current state of the art, J. Mater. Sci. 42 (2007) 2917-2933.
[6] J. M. Hernández, B. Middendorf, M. Gehrke, H. Budelmann, Use of wastes of the sugar industry as pozzolana in lime-pozzolana binders: study of the reaction, Cem. Concr. Res. 28 (1998) 1525-1536.
[7] D. G. Nair, A. Fraaij, A. A. Klaassen, A. P. Kentgens, A structural investigation relating to the pozzolanic activity of rice husk ashes, Cem. Concr. Res. 38 (2008) 861-869.
[8] N. N. Yeboah, C. R. Shearer, S. E. Burns, K. E. Kurtis, Characterization of biomass and high carbon content coal ash for productive reuse applications, Fuel. 116 (2014) 438-447.
[9] G. C. Cordeiro, R. D. Toledo Filho, E. M. R. Fairbairn, Use of ultrafine rice husk ash with high-carbon content as pozzolan in high performance concrete, Mater. Struct. 42 (2009) 983-992.
[10] J. M. Medina, I. F. S. del Bosque, M. Frías, M. S. de Rojas, C. Medina, Characterisation and valorisation of biomass waste as a possible addition in eco-cement design, Mater. Struct. 50 (2017) 207.
[11] P. K. Mehta, N. Pitt, Energy and industrial materials from crop residues, Res. Recov. Cons. 2 (1976) 23-38.
[12] T. Poinot, M. E. Laracy, C. Aponte, H. M. Jennings, J. A. Ochsendorf, E. A. Olivetti, Beneficial use of boiler ash in alkali-activated bricks, Res. Cons. Recycl. 128 (2018) 1-10.
[13] P. Chaunsali, H. Uvegi, R. Osmundsen, J. A. Ochsendorf, E. A. Olivetti, Mineralogical and Microstructural Characterization of Biomass Ash Binder, Cem. Concr. Compos. 89 (2018) 41-51.
[14] E. Freeman, Y-M Gao, R. Hurt, E. Suuberg, Interactions of carbon-containing fly ash with commercial air-entraining admixtures for concrete, Fuel. 76 (1997) 761-765.
[15] S. Wang, A. Miller, E. Llamazos, F. Fonseca, L. Baxter, Biomass fly ash in concrete: mixture proportioning and mechanical properties, Fuel. 87 (2008) 365-371.
[16] I.S. 1077, Indian Standard for Common Burnt Clay Building Bricks – Specification (1992).
[17] A. W. Harris, M. C. Manning, W. M. Tearle, C. J. Tweed, Testing of models of the dissolution of cements—leaching of synthetic CSH gels, Cem. Concr. Res. 32 (2002)731-746.
[18] S. W. Swanton, T. G. Heath, A. Clacher, Leaching behaviour of low Ca:Si ratio $CaO–SiO_2–H_2O$ systems, Cem. Concr. Res. 88 (2016) 82-95.
[19] H. Stade, On the reaction of CSH (di, poly) with alkali hydroxides, Cem. Concr. Res. 19 (1989) 802-810.
[20] E. L'Hôpital, B. Lothenbach, K. Scrivener, D. Kulik, Alkali uptake in calcium alumina silicate hydrate (CASH), Cem. Concr. Res. 85 (2016)122-136.
[21] S-Y Hong, F. Glasser, Alkali binding in cement pastes: Part I. The CSH phase, Cem. Concr. Res. 29 (1999) 1893-1903.
[22] N Schiopu, L. Tiruta-Barna, E. Jayr, J. Méhu, P. Moszkowicz, Modelling and simulation of concrete leaching under outdoor exposure conditions, Sci. Total Environ. 407 (2009) 1613-1630.
[23] C. Carde, R. François, Modelling the loss of strength and porosity increase due to the leaching of cement pastes, Cem. Concr. Compos. 21 (1999) 181-188.

[24] M. Jebli, F. Jamin, C. Pelissou, E. Malachanne, E. Garcia-Diaz, M.S. El Youssoufi, Leaching effect on mechanical properties of cement-aggregate interface, Cem. Concr. Compos. 87 (2018) 10-19.
[25] F. Rajabipour, E. Giannini, C. Dunant, J.H. Ideker, M.D.A. Thomas, Alkali–silica reaction: Current understanding of the reaction mechanisms and the knowledge gaps, Cem. Concr. Res. 76 (2015) 130-146.
[26] M. E. Laracy, Valorization of boiler ash in alkali activated material, M.S. Dissertation, Massachusetts Institute of Technology, 2015.
[27] J. Zhang, Scherer, G. W., Comparison of methods for arresting hydration of cement, Cem. Concr. Res. 41(10) (2011) 1024-1036.
[28] M.C.G. Juenger, H. M. Jennings, The use of nitrogen adsorption to assess the microstructure of cement paste, Cem. Concr. Res. 31(6) (2001) 883-892.
[29] Collier, N. C., J. H. Sharp, N. B. Milestone, J. Hill, I. H. Godfrey, The influence of water removal techniques on the composition and microstructure of hardened cement pastes, Cem. Concr. Res. 38, no. 6 (2008) 737-744.
[30] Ruben Snellings, Jacek Chwast, Özlem Cizer, Nele De Belie, Yuvaraj Dhandapani, Pawel Durdzinski, Jan Elsen et al. Report of TC 238-SCM: hydration stoppage methods for phase assemblage studies of blended cements—results of a round robin test, Materials and Structures 51(4) (2018) 111.
[31] T. Bach, E. Chabas, I. Pochard, C. C. D. Coumes, J. Haas, F. Frizon, A. Nonat, Retention of alkali ions by hydrated low-pH cements: Mechanism and Na^+/K^+ selectivity, Cem. Concr. Res. 51(2013) 14-21.
[32] Z. Zhang, J. L. Provis, A. Reid, H. Wang, Fly ash-based geopolymers: the relationship between composition, pore structure and efflorescence, Cem. Concr. Res. 64 (2014) 30-41.
[33] C. Shi, J. Stegemann, Acid corrosion resistance of different cementing materials, Cem. Concr. Res. 30 (2000) 803-808.
[34] P. Scherrer, Bestimmung der Grösse und der inneren Struktur von Kolloidteilchen mittels Röntgenstrahlen, Nachr. Ges. Wiss. Göttingen. 26 (1918) 98-100.
[35] J.I. Langford and A.J.C. Wilson, Scherrer after Sixty Years: A Survey and Some New Results in the Determination of Crystallite Size, J. Appl. Cryst. 11 (1978) 102-113.
[36] P. Yu, R. J. Kirkpatrick, B. Poe, P. F. McMillan, X. Cong, Structure of calcium silicate hydrate (C-S-H): Near-, Mid-, and Far-infrared spectroscopy, J. Am. Ceram. Soc. 82 (1999) 742-748.
[37] H.F.W. Taylor, Cement Chemistry, 2nd Edition, Thomas Telford, 1997.
[38] A. Hidalgo, S. Petit, C. Domingo, C. Alonso, C. Andrade, Microstructural characterization of leaching effects in cement pastes due to neutralisation of their alkaline nature: Part I: Portland cement pastes, Cem. Concr. Res. 37 (2007) 63-70.